Article ID: 1006-8775(2004) 02-0123-10

THREE-DIMENSIONAL VARIABLES ALLOCATION IN MESOSCALE MODELS

LIU Yu-di (刘宇迪)[1, 2] and LU Han-cheng (陆汉城)[2]

(1. *LASG*, *Institute of Atmospheric Physics*, *Chinese Academy of Sciences*, *Beijing* 100029 *China*;
2. *Meteorological College*, *PLA University of Science and Technology*, *Nanjing* 211101, *China*)

ABSTRACT: Forecasts and simulations are varied owing to different allocation of 3-dimensional variables in mesoscale models. No attempts have been made to address the issue of optimizing the simulation with a 3-dimensional variables distribution that should come to be. On the basis of linear nonhydrostatic anelastic equations, the paper hereby compares, mainly graphically, the computational dispersion with analytical solutions for four kinds of 3-dimensional meshes commonly found in mesoscale models, in terms of frequency, horizontal and vertical group velocities. The result indicates that the 3-D mesh C/CP has the best computational dispersion, followed by Z/LZ and Z/LY, with the C/L having the worst performance. It is then known that the C/CP mesh is the most desirable allocation in the design of nonhydrostatic baroclinic models. The mesh has, however, larger errors when dealing with shorter horizontal wavelengths. For the simulation of smaller horizontal scales, the horizontal grid intervals have to be shortened to reduce the errors. Additionally, in view of the dominant use of C/CP mesh in finite-difference models, it should be used in conjunction with the Z/LZ or Z/LY mesh if variables are allocated in spectral models.

Key words: 3-D variable allocation; mesoscale models; frequency; group velocity; nonhydrostatic; anelastic approximation

CLC number: P456.7 **Document code:** B

1 INTRODUCTION

It is well known that the mesoscale weather phenomena badly threaten people lives and social production. Now many meteorologists use numerical models to predict and simulate them. The horizontal variables allocation in the mesoscale models were studied by Winninghoff[1] and Arakawa[2], then following the idea of Winninghoff, Liu[3-6] again systematically researched all existing horizontal grids, indicating that the Arakawa C, Z and Eliassen grids have the best computational performance. And Liu [7-10] also performed a study of vertical variables allocation in the case of nonhydrostatic models, asserting that L, CP, LZ and LY grids have better computational dispersion properties. Then, which of the 3D grids consisting of better horizontal and vertical grids is the best remains unsolved hitherto, in particular in the case of the nonhydrostatic models, a problem that has been ignored by many investigators. To supply the gap in terms of frequency, horizontal group velocity and vertical group velocity using the anelastic approximation equations the present paper is intended to deal with dispersion properties in the 3D grids (C/L, C/CP, Z/LZ and Z/LY) consisting of better horizontal grids (C, Z) and better vertical meshes (L, CP, LZ and LY) in the respect of the computational dispersion properties whereby some better 3D grids are chosen out of the study grids for the reference of model

Received date: 2003-02-28; **revised date:** 2004-08-18
Foundation item: Supported by the open research program of LASG, Institute of Atmospheric Physics, Chinese Academy of Sciences
Biography: LIU Yu-di (1971 –), male, associate professor, Ph.D., native from Inner Mongolian Autonomous Region, undertaking data assimilation and ocean remote sensing study.

designers. Though the Eliassen grid has better computational dispersion properties, it is time-staggered one, and there are many difficulties when it is used in the practical model. So few models use it, and in the paper it is not discussed either.

To integrally present calculated dispersions from 4 kinds of 3D grids we structure the study in the following way. Section 2 shows an analytical dispersion equation, analytical horizontal and vertical group velocity equations of linear anelastic adaptive equations. Given in Section 3 are the difference expressions, numerical dispersion and group velocity equations for the 4 kinds of 3D grids, and graphically compared with analytical ones. Their computational dispersions are discussed in Section 4, with concluding remarks shown in Section 5.

2 DIFFERENTIAL CASE

To study the 3D variable allocation in mesoscale models, we begin from the nonhydrostatic anelastic equations.

$$\frac{\partial u}{\partial t}+\frac{\partial P}{\partial x}-fv=0\,,$$
$$\frac{\partial v}{\partial t}+\frac{\partial P}{\partial y}+fu=0\,,$$
$$\frac{\partial w}{\partial t}+\frac{\partial P}{\partial z}-g\theta=0\,,$$
$$\frac{\partial \theta}{\partial t}+Sw=0\,,$$
$$\frac{\partial u}{\partial x}+\frac{\partial v}{\partial y}+\frac{\partial w}{\partial z}=0\,. \tag{1}$$

Specifically u, v and w are velocity components in the x, y and z directions, respectively, $p(x,y,z,t)=\overline{p}(z)+p'(x,y,z,t)$ stands for pressure that is divided into a hydrostatic basic-state component $\overline{p}$ and a disturbance one p'; ρ for air density, with $P=p'/\rho_0$, the denominator being a steady ρ under the Boussinesq approximation; $\Theta(x,y,z,t)=\overline{\Theta}(z)+\Theta'(x,y,z,t)$ for potential temperature, which is separated into a basic state $\overline{\Theta}$ and a disturbance component Θ'; $S(z)=d\left(\ln\overline{\Theta}\right)/dz$; $\theta=\Theta'/\Theta_0$, the denominator being a steady $\overline{\Theta}$; g for gravitational acceleration; f for the steady Coriolis parameter.

We now assume a wave equation of the form

$$F=\overline{F}e^{i(kx+my+lz-\omega t)}\,, \tag{2}$$

in which $k=2\pi/L_x$, $m=2\pi/L_y$ and $l=2\pi/L_z$, with L_x, L_y and L_z standing for wave number and length in the *x*, *y* and *z* directions, respectively, ω the frequency.

The wave solution Eq.(2) is then inserted into Eqs.(1), leading to an analytical dispersion relation

$$\left(\frac{\omega}{f}\right)_{diff}^2=\frac{\ell^2+\lambda^2\left(k^2+m^2\right)}{k^2+m^2+\ell^2} \tag{3}$$

where $\lambda = \sqrt{gS}\big/ f$ is the Rossby deformation radius.

From Eq.(3) we derive a horizontal group velocity components (denoted hereinafter as HGV) and the vertical counterpart (VGV). Since inertia gravitational waves described in Eq.(1) is isotropic, the assumption of $k = m$ has no influence on the conclusion to arrive at, thus allowing the x-axis HGV to represent the y-axis equivalent as well. That is to say, there is only a horizontal group velocity component, i.e. the group velocity components in the x direction.

$$\text{HGV}=\frac{f\left(\dfrac{4k\lambda^2}{2k^2+l^2}-\dfrac{4k(l^2+2k^2\lambda^2)}{(2k^2+l^2)^2}\right)}{2\sqrt{\dfrac{l^2+2k^2\lambda^2}{2k^2+l^2}}},$$

$$\text{VGV}=\frac{f\left(\dfrac{2l}{2k^2+l^2}-\dfrac{2l(l^2+2k^2\lambda^2)}{(2k^2+l^2)^2}\right)}{2\sqrt{\dfrac{l^2+2k^2\lambda^2}{2k^2+l^2}}}.$$

We shall compare the dispersion features from a range of 3D grids based upon the change in frequency and group velocity.

3 3D GRIDS

In the section we study the computational dispersion features of the 3D grids (C/L, C/CP, Z/LZ and Z/LY) shown in Fig.1 that consist of better horizontal grids (C, Z) and better vertical ones (L, CP, LZ and LY) to investigate dispersions dominantly from the perspective of frequency and group velocity components (HGV and VGV).

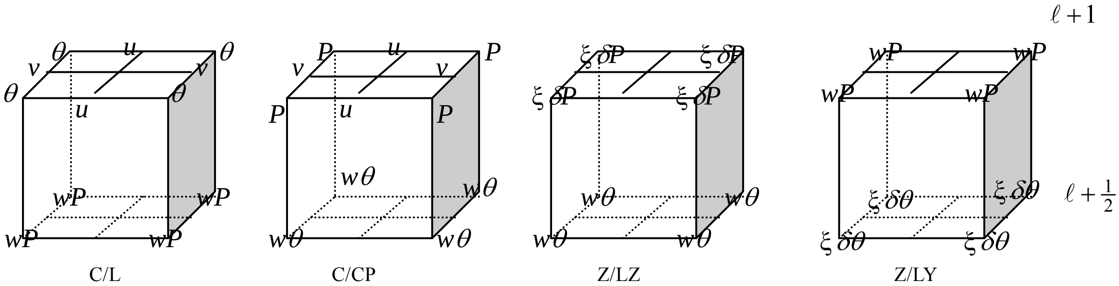

Fig.1 Allocation of variables for individual 3D grids.

3.1 *C/L Grid*

The nonhydrostatic anelastic Eqs.(1), when employed in the C/L grid, has, through the Shuman operator, the following form

$$\frac{\partial u}{\partial t}+\overline{P}_x^z-f\overline{v}^{xy}=0,$$

$$\frac{\partial v}{\partial t}+\overline{P}_y^z+f\overline{u}^{xy}=0,$$

$$\frac{\partial \mathrm{w}}{\partial \mathrm{t}} + \overline{\mathrm{P}}_{\mathrm{z}}^{\mathrm{z}} - \mathrm{g}\overline{\theta}^{\mathrm{z}} = 0,$$
$$\frac{\partial \theta}{\partial \mathrm{t}} + \mathrm{S}\overline{\mathrm{w}}^{\mathrm{z}} = 0,$$
$$\mathrm{u}_{\mathrm{x}} + \mathrm{v}_{\mathrm{y}} + \mathrm{w}_{\mathrm{z}} = 0. \tag{4}$$

Set Eqs.(4) to have its solution

$$F = \hat{F}\exp[i(k\kappa\Delta x + m\mu\Delta y + \ell\rho\Delta \mathrm{z} - \omega t)], \tag{5}$$

with k, μ and ρ as positive integers.

Eq.(5) is substituted into Eqs.(4), giving

$$\left(\frac{\omega}{f}\right)^2_{C/L} = \frac{\cos^2\frac{k\Delta x}{2}\cos^2\frac{m\Delta y}{2}\left(\frac{\sin\frac{\ell\Delta \mathrm{z}}{2}}{\frac{\Delta \mathrm{z}}{2}}\right)^2 + \lambda^2\cos^2\frac{\ell\Delta \mathrm{z}}{2}\left(\left(\frac{\sin\frac{k\Delta x}{2}}{\frac{\Delta x}{2}}\right)^2 + \left(\frac{\sin\frac{m\Delta y}{2}}{\frac{\Delta y}{2}}\right)^2\right)}{\left(\frac{\sin\frac{k\Delta x}{2}}{\frac{\Delta x}{2}}\right)^2 + \left(\frac{\sin\frac{m\Delta y}{2}}{\frac{\Delta y}{2}}\right)^2 + \left(\frac{\sin\frac{\ell\Delta \mathrm{z}}{2}}{\frac{\Delta \mathrm{z}}{2}}\right)^2}$$

Since the group velocity equations (with HGV and VGV omitted) are very complicated and don't show any available information, they are not listed in the paper. Here they are mentioned so that they will be graphically compared with analytical ones in section 4. So do other grids hereinafter.

3.2 *C/CP Grid*

Put into use in the this grid, the nonhydrostatic anelastic Eqs.(1) has the form

$$\frac{\partial \mathrm{u}}{\partial \mathrm{t}} + \mathrm{P}_{\mathrm{x}} - \mathrm{f}\overline{\mathrm{v}}^{\mathrm{xy}} = 0,$$
$$\frac{\partial \mathrm{v}}{\partial \mathrm{t}} + \mathrm{P}_{\mathrm{y}} + \mathrm{f}\overline{\mathrm{u}}^{\mathrm{xy}} = 0,$$
$$\frac{\partial \mathrm{w}}{\partial \mathrm{t}} + \mathrm{P}_{\mathrm{z}} - \mathrm{g}\theta = 0,$$
$$\frac{\partial \theta}{\partial \mathrm{t}} + \mathrm{S}\mathrm{w} = 0,$$
$$\mathrm{u}_{\mathrm{x}} + \mathrm{v}_{\mathrm{y}} + \mathrm{w}_{\mathrm{z}} = 0,$$

whose formulations of dispersion are given as

$$\left(\frac{\omega}{f}\right)^2_{C/CP} = \frac{\cos^2\frac{k\Delta x}{2}\cos^2\frac{m\Delta y}{2}\left(\frac{\sin\frac{\ell\Delta z}{2}}{\frac{\Delta z}{2}}\right)^2 + \lambda^2\left(\left(\frac{\sin\frac{k\Delta x}{2}}{\frac{\Delta x}{2}}\right)^2 + \left(\frac{\sin\frac{m\Delta y}{2}}{\frac{\Delta y}{2}}\right)^2\right)}{\left(\frac{\sin\frac{k\Delta x}{2}}{\frac{\Delta x}{2}}\right)^2 + \left(\frac{\sin\frac{m\Delta y}{2}}{\frac{\Delta y}{2}}\right)^2 + \left(\frac{\sin\frac{\ell\Delta z}{2}}{\frac{\Delta z}{2}}\right)^2}.$$

HGV and VGV are omitted.

3.3 *Z/LZ Grid*

In this case, from the nonhydrostatic anelastic Eqs.(1) we derive a system of equations denoted by vorticity and divergence, i.e.,

$$\begin{gathered}
\frac{\partial \delta}{\partial t} + \nabla^2 P - f\xi = 0, \\
\frac{\partial \xi}{\partial t} + f\delta = 0, \\
\frac{\partial w}{\partial t} + \frac{\partial P}{\partial z} - g\theta = 0, \\
\frac{\partial \theta}{\partial t} + Sw = 0, \\
\delta + \frac{\partial \omega}{\partial z} = 0.
\end{gathered} \tag{6}$$

By virtue of a variables configuration scheme for the study grid (Fig.1) discrete equations are as follows.

$$\begin{gathered}
\frac{\partial \delta}{\partial t} + P_{xx} + P_{yy} - f\xi = 0, \\
\frac{\partial \xi}{\partial t} + f\delta = 0, \\
\frac{\partial w}{\partial t} + P_z - g\theta = 0, \\
\frac{\partial \theta}{\partial t} + Sw = 0, \\
\delta + w_z = 0.
\end{gathered}$$

Into which Eq.(5) is substituted, resulting in formulations of dispersion properties as follows:

$$\left(\frac{\omega}{f}\right)^2_{Z/LZ}=\frac{\left(\frac{\sin\frac{\ell\Delta z}{2}}{\frac{\Delta z}{2}}\right)^2+\lambda^2\left(\left(\frac{\sin\frac{k\Delta x}{2}}{\frac{\Delta x}{2}}\right)^2+\left(\frac{\sin\frac{m\Delta y}{2}}{\frac{\Delta y}{2}}\right)^2\right)}{\left(\frac{\sin\frac{k\Delta x}{2}}{\frac{\Delta x}{2}}\right)^2+\left(\frac{\sin\frac{m\Delta y}{2}}{\frac{\Delta y}{2}}\right)^2+\left(\frac{\sin\frac{\ell\Delta z}{2}}{\frac{\Delta z}{2}}\right)^2}.$$

HGV and VGV are also omitted

3.4 *Z/LY Grid*

For this mesh Eq.(6) is discretized as

$$\frac{\partial\delta}{\partial t}+\overline{P}^z_{xx}+\overline{P}^z_{yy}-f\xi=0,$$

$$\frac{\partial\xi}{\partial t}+f\delta=0,$$

$$\frac{\partial w}{\partial t}+\overline{P}^z_z-g\overline{\theta}^z=0,$$

$$\frac{\partial\theta}{\partial t}+S\overline{w}^z=0,$$

$$\delta+w_z=0.$$

Leading to the dispersion features denoted by

$$\left(\frac{\omega}{f}\right)^2_{Z/LY}=\frac{\left(\frac{\sin\frac{\ell\Delta z}{2}}{\frac{\Delta z}{2}}\right)^2+\lambda^2\cos^2\frac{\ell\Delta z}{2}\left(\left(\frac{\sin\frac{k\Delta x}{2}}{\frac{\Delta x}{2}}\right)^2+\left(\frac{\sin\frac{m\Delta y}{2}}{\frac{\Delta y}{2}}\right)^2\right)}{\left(\frac{\sin\frac{k\Delta x}{2}}{\frac{\Delta x}{2}}\right)^2+\left(\frac{\sin\frac{m\Delta y}{2}}{\frac{\Delta y}{2}}\right)^2+\left(\frac{\sin\frac{\ell\Delta z}{2}}{\frac{\Delta z}{2}}\right)^2}$$

HGV and VGV are also omitted

4 DISCUSSIONS

The dispersion characteristics calculated in the different grids (see Section 3) are too complicated to be compared in a direct manner such that a graphic representation is prepared for this purpose. Fig.2 portrays the frequencies from all the 3D grids versus that from analytical treatment.

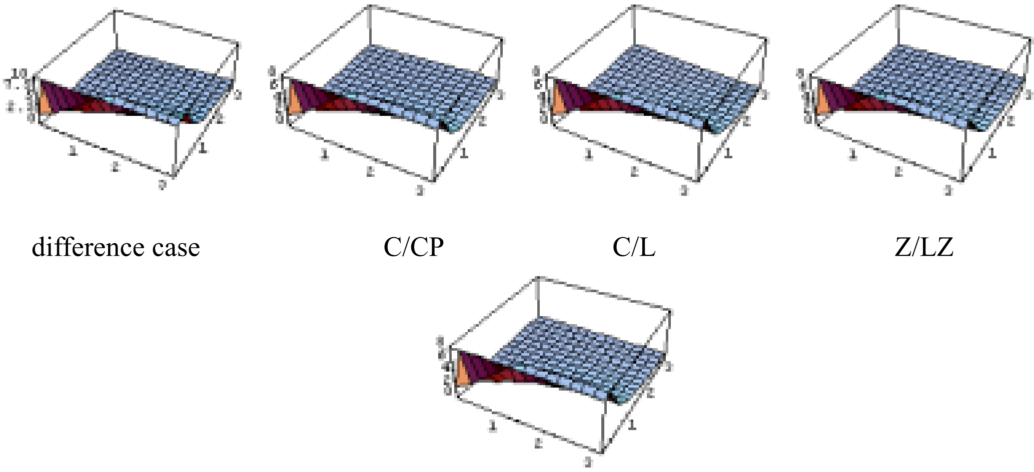

Fig.2. Variations of frequencies from the 3D grids. The *x*-axis coordinate is $k\Delta x$, the *y*-axis one is $\ell\Delta Z$ and the *z*-axis is ω/f.

We notice therefrom that the frequencies obtained from the grids and analytical treatment are fundamentally identical except for the range in value, which is somewhat different from the latter. To further illustrate their discrepancies we present relative errors *R* of frequencies from the grids relative to that of analytical solution

$$R_j^i = \frac{C_j^i - C_j^{diff}}{C_j^{diff}}$$

where the superscripts *i* and *diff* denote a type of the grids and the differential case, respectively, and the subscript the calculated frequency and group velocity (HGV and VGV).

Fig.3 delineates the relative errors of frequencies, indicating smaller magnitudes for Z/LZ and C/CP cases. The maximal error is 30% on the C/CP grid and 20% on the Z/LZ grid, respectively, however, it is up to 100% on the C/L grid. With the shortening of the horizontal wave length, the error on the C/CP is increasing, but it is insensitive to the change of the vertical wave length, i.e. for the horizontal short wave, its error is relatively larger. While on the Z/LZ grid there are larger errors for the horizontal short wave and vertical long wave. As a result, the Z/LZ and C/CP grids have the best dispersion properties from the perspective of the frequency.

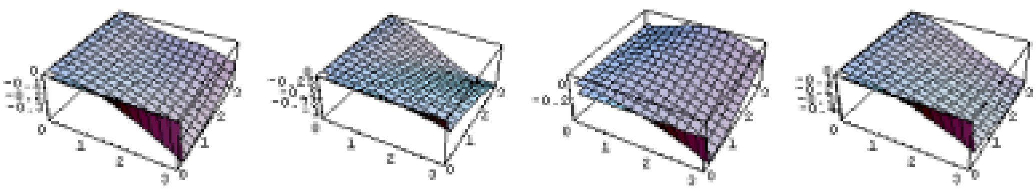

C/CP C/L Z/LZ Z/LY

Fig.3. Relative errors (ordinate) for the frequencies of grids with respective to analytical solution, with the same horizontal coordinates as in Fig.2.

Fig.4 presents the horizontal group velocity component (HGV) from these 3D grids. One sees therefrom no pronounced difference in their results and the trend in rough conformity with that of analytically obtained frequency except rather big discrepancy in the range of value. Their relative errors are shown in Figs.5 that illustrates small difference for the cases of C/CP, Z/LY and C/L grids – so small as to be mostly within the bound of 100%. The wave band range producing larger error on C/CP grid is in the horizontal short wave part, the horizontal long wave and vertical short wave part, however, on the Z/LZ grid, it is both in the horizontal and vertical short wave part. It follows that the C/CP and Z/LY grids yield quite good dispersion properties, as viewed from HGV.

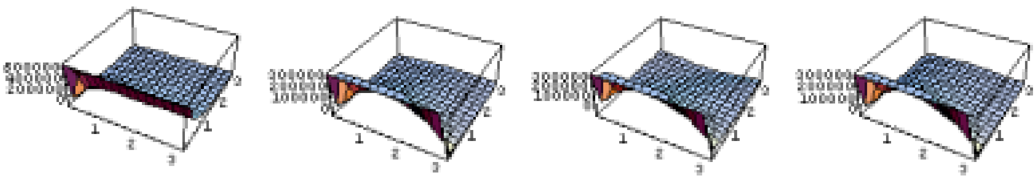

Difference case C/CP C/L Z/LZ

Z/LY

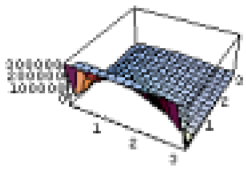

Fig.4. HGV from all these grids, with the ordinate denoted by C_g / f. Otherwise as in Fig.2.

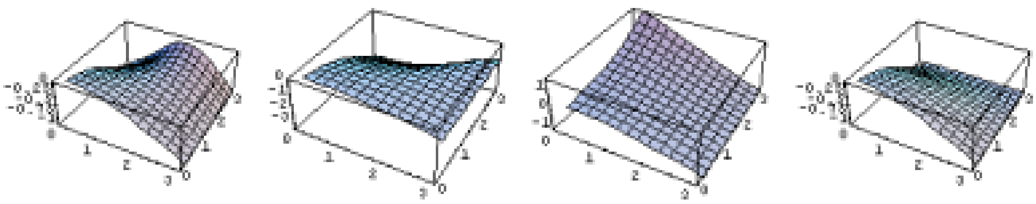

C/CP C/L Z/LZ Z/LY

Fig.5. Relative errors (ordinate) of HGV (grid with respect to analytical results), with the same horizontal coordinates as in Fig.2.

Now let us have a look at the vertical group velocity component (VGV) from all the grids (Fig.6), where no very big difference occurs, with the varying trends being basically the same as that of the analytical solution except the range of magnitude, which of the C/CP and C/L grids are the closest to that of the analytical solution. Likewise, their relative errors with respect to analytical solution are given in Figs.7 that illustrates small relative errors for each of the cases of C/CP, Z/LZ and Z/LY – so small as to fall inside 100% in the vertical short wave band. We thus see that these grids give good dispersion feature, as viewed from the perspective of VGV.

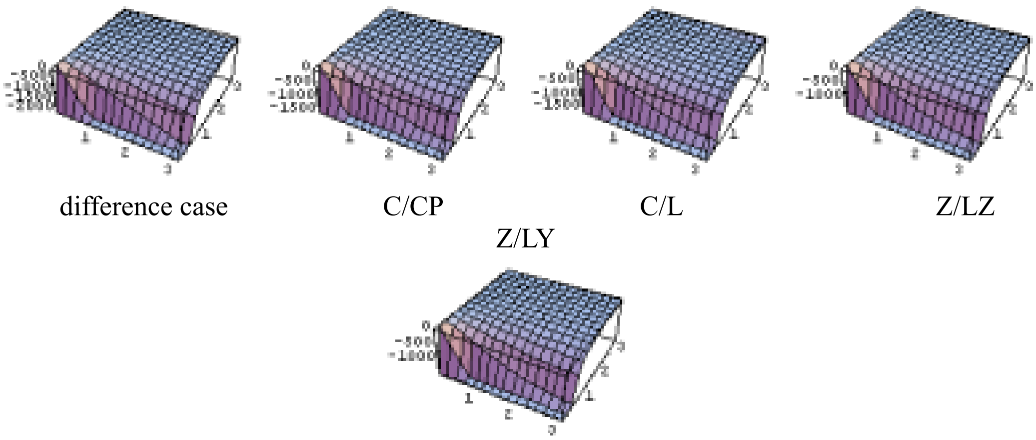

Fig.6. VGV from the grids with C_g / f on the ordinate. Otherwise as in Fig.2.

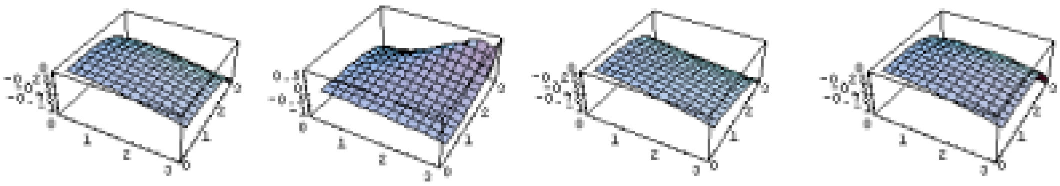

Fig.7. Relative error (ordinate) of VGV with respect to analytical treatment, with the same horizontal coordinates as in Fig.2.

Now we deal with the cause of the difference in value between grid findings and analytical solution. It is known that when a system of differential equations is discretized in a range of grids, the number of "mean quantities" terms, ad hoc ones over the difference term, in the transformed equations are responsible for value of error, and the less the terms, the closer the solution to that of the original equations and vice verse. Of course the more averaging in the vertical dimension lead to the decrease of accurateness in the same direction, and the smaller the scale of the wave is, the larger the errors are, so does it in the horizontal direction. Now we revert to the discretized expressions in all the grids (Section 3)

(1) C/L grid needs vertical averaging over the horizontal pressure gradient force, horizontal one over the horizontal velocity in the Coriolis term. In particular, the former is one over the difference so that it causes larger error.

(2) C/CP grid has better dispersion properties since it involves no "mean " quantities except the horizontal one over the Coriolis term

(3) Z/LZ grid seems no averaging, but P_{xx} and P_{yy} are equivalent to three-point smoothing, that is to say, they are also mean quantities, thereby leading to errors contained in it.

(4) Z/LY grid is inferior to Z/LZ from the aspect of dispersion properties because many terms are vertically averaged on it.

We find the number of 'means' terms related to Z/LZ and C/CP are the minimum, thereby making for better dispersion properties compared to the others.

5 CONCLUDING REMARKS

From the foregoing analysis we come to the following conclusions.

a. Viewed from the frequency, HGV and VGV change in combination, the C/CP grid is able to yield quite exact simulation of inertia gravitational waves, followed by Z/LZ and Z/LY, with the C/L having the worst performance. In developing a nonhydrostatic baroclinic model, therefore, it is suggested that the C/CP grid be adopted as much as possible.

b. The C/CP finds its use dominantly in a limited difference model and in considering the configuration (or arrangement) for a spectral model; the C/CP grid should be combined with the Z/LZ grid or Z/LY grid.

(3) The C/CP mesh has larger errors when dealing with shorter horizontal wavelengths. For the simulation of smaller horizontal scales, the horizontal grid intervals have to be shortened to reduce the errors.

(4) When using Z/LZ grid to simulate the waves with shorter horizontal and longer vertical wavelength, the horizontal (vertical) grid spacing has to be shortened (lengthened) to reduce the error.

(5) Since the Z/LY grid has larger error at shorter horizontal and vertical wave band, the horizontal and vertical grid spacing have to be shorter when adopting the Z/LY grid.

REFERENCES:

[1] Winninghoff F J. On the adjustment towards a geostrophic balance in a simple primitive equation model with application to the problems and objective analysis [M]. Ph. D. thesis, University of California, Los Angeles, 1968.

[2] ARAKAWA A, LAMB V R. Computational dynamic processes of UTLA general circulation model [A]. Methods in Computational Physics [M]. CHANG J Ed., Academic Press, 1977. 173-256.

[3] LIU Yu-di. Study on dispersion features as calculated in horizontal grids [J], *Quarterly Journal of Applied Meteorology*, 2001,**12**(2): 140-149.

[4] LIU Yu-di. Effects of horizontal grids on Rossby wave [J]. *Acta Meteorologica Sinica*, 2002, **60**(1): 76-84.

[5] LIU Yu-di. Research on atmospheric motion in horizontal discrete grids [J]. *Advances in Atmospheric Sciences*, 2003, **20**(1): 139-148.

[6] WANG Ju, LIU Yu-di. Impact of horizontal grid on geostrophic evolution simulating [J]. *Journal of Tropical Meteorology*, 2003, **19**(3): 323-328.

[7] LIU Yu-di, ZHU Hong-wei. Study on dispersion features as calculated in vertical grids [J]. *Quarterly Journal of Applied Meteorology*, 2001, **12**(3): 348-357.

[8] LIU Yu-di, JI Zhong-zhen, et al. Comparative study of dispersion features based on a range of vertical staggered grids [J]. *Scientia Atmospherica Sinica*, 2001, **25**(4): 523-535.

[9] LIU Yu-di, CHEN Xiao-ping. Vertical distribution of field variables and simulation of gravity-inertial wave [J]. *Journal of PLA University of science and technology*, 2001, **2**(6): 86-89.

[10] LIU Yu-di, JI Zhong-zhen, WANG Bin. Study on computational properties of several vertical grids with a nonhydrostatic model in comparison to analytical solutions [J]. *Advances in Atmospheric Sciences*, 2002, **19**(3): 528-543.